JOURNAL OF MATERIALS SCIENCE 24 (1989) 343–348

Electrical properties and internal friction in vanadium phosphate glasses

T. TSUCHIYA, M. OTONARI
Department of Industrial Chemistry, Faculty of Science and Technology, Science University of Tokyo, Noda, Chiba, 278, Japan

The electrical properties and internal friction in the glasses of $(50–80)V_2O_5 \cdot (50–20)P_2O_5$ and $70V_2O_5 \cdot xB_2O_3 \cdot (30 - x)P_2O_5$ were measured. In both system glasses, one peak on internal friction was observed in the temperature range of −100 to 200° C at a frequency of about 1 Hz. The area of the internal friction peak increased with increasing valence ratio R, similar to those in the d.c. conductivity and dielectric increment. Frequency temperature dependence of dielectric loss peak and peak on internal friction showed a parallel line, and its activation energy was 0.33 eV. From the above results, the peak observed at internal friction was due to the hopping of localized electrons in small polarons.

1. Introduction

It is well known that phosphate glasses with high vanadium content show typical electrical hopping having high conductivity [1–8]. The d.c. conductivity of vanadium phosphate glasses shows a maximum value when the valence ratio of vanadium ion R ($R = V^{4+}/V^{4+} + V^{5+}$) is 0.1–0.2. This specific phenomenon is not yet clear. To clarify the mechanism of such conductivity, the measurement of dielectric relaxation is useful, as the short distance transition of electric charge can be analysed. However, the measurement of dielectric relaxation requires very difficult techniques, especially in the range of ultra low frequency. In contrast, the measurement of internal friction is so easy in this frequency range that the behaviour of electric charge can be directly identified at a frequency of around 1 Hz. Many research reports are available on the measurement of internal friction regarding alkali-containing glasses [9–11]. However, few reports are available regarding electronic conduction glasses containing transition metal oxide [12–18]. We arranged instruments for precision measurement of internal friction in our research, and also developed an automatic control system by the aid of computer. In this research, we measured the electrical properties (d.c. conductivity, dielectric relaxation) and internal friction in the glasses of vanadium phosphate and vanadium borophosphate. Further examinations were conducted on the correlation between internal friction and electrical properties.

2. Experimental procedure

2.1. Preparation of specimens

Both reagents of V_2O_5 and H_3PO_4 were of special high grade. They were blended in a ratio so as to make a composition of $(50–80)V_2O_5 \cdot (50–20)P_2O_5$ and $70V_2O_5 \cdot xB_2O_3 \cdot (30 - x)P_2O_5$, charged in an alumina crucible, calcined and then melted at 1200° C for 2 h. Melted glasses were cast in a stainless steel disc-shaped mould with a diameter of 40 mm and a thickness of 3 to 4 mm. After releasing the strain, the disc-shaped glasses were polished on both sides and three gold electrodes were attached using the vapour deposition process. These were the specimens for the measurement of electric properties. Another type of specimen used for the measurement of internal friction was fibre-shaped with a diameter of 1 mm and a length of 40 mm, and was produced by extracting a quartz rod from the melted glass in the alumina crucible.

2.2. Measurements of d.c. conductivity and dielectric properties

Direct current (d.c.) conductivity was measured by current–voltage methods by using a vibrating reed d.c. amplifier and the a.c. conductivity was measured in the frequency range of 30 to 10^6 Hz by means of a transformer bridge. Measuring methods and treatments of measured data were the same with those in our previous report [17, 18].

2.3. Measurements of internal friction

A counter-suspension type torsion pendulum apparatus was used to measure internal friction [17, 18]. The oscillation was detected by the detection coils, amplified by a differential amplifier, (read by A–D converter) and recorded on disc after calculating the logarithmic decrement (Δ) and cycle time (T_d) by means of computer.

2.4. Valence analysis of vanadium

The glass sample was crushed fine enough to pass through a 400 mesh, and a predetermined amount was dissolved in a hot hydrosulphlic acid (1 + 1) solution. By a redox reaction titration with $KMnO_4$, the valence ratio of the vanadium ion ($R = V^{4+}/V^{4+} + V^{5+}$) was determined. Hereafter, the valence ratio of the vanadium will be abbreviated as the R ratio.

0022–2461/89 $03.00 + .12

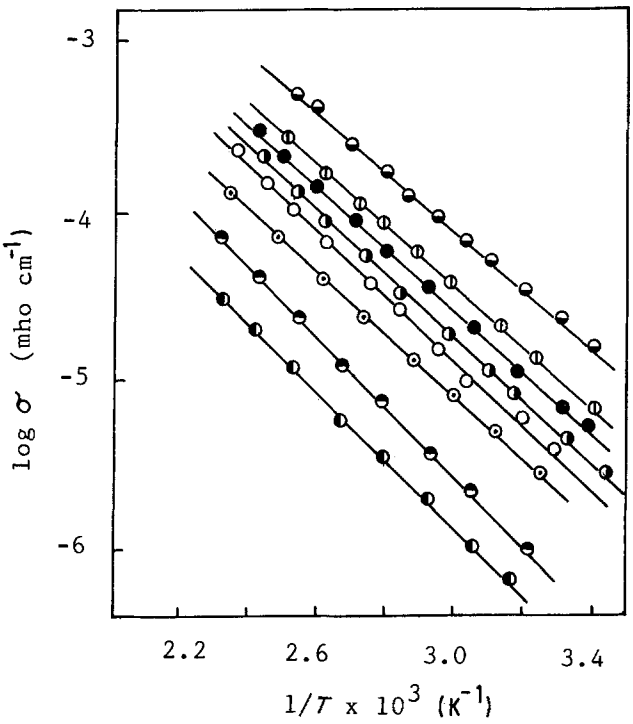

Figure 1 Temperature dependence of d.c. conductivity in the glasses of $xV_2O_5 \cdot (100 - x)P_2O_5$ and $70V_2O_5 \cdot xB_2O_3 \cdot (30 - x)P_2O_5$ series. (◒ $y = 15$, ◑ $y = 10$, ● $y = 7$, ◑ $y = 5$, ○ $y = 2$, ⊙ $x = 70$, ◓ $x = 60$, ◐ $x = 50$).

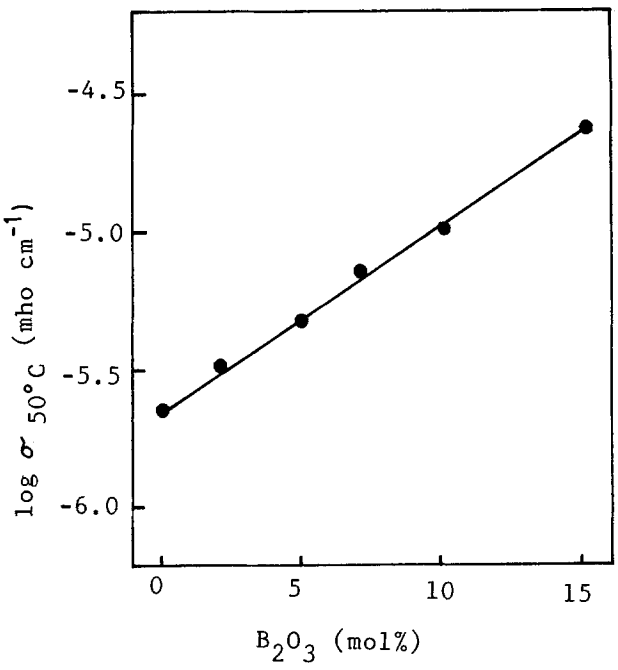

Figure 2 Compositional dependence of d.c. conductivity at 50° C for the glasses of $70V_2O_5 \cdot yB_2O_3 \cdot (30 - x)P_2O_5$.

3. Experimental results and discussions

3.1. D.C. conductivity

Fig. 1 shows the temperature dependence of d.c. conductivity in the glasses of $(50–80)V_2O_5 \cdot (50–20)P_2O_5$ system. All of the specimens satisfied the following Equation

$$\sigma = \sigma_0 \exp\left(-\frac{\Delta H_{dc}}{RT}\right) \quad (1)$$

where σ_0 is a pre-exponential factor, R the gas constant and ΔH_{dc} the activation energy of d.c. conductivity. The d.c. conductivity increased with increasing V_2O_5 content. On the other hand the conductivity in the glasses of $70V_2O_5 \cdot xB_2O_3 \cdot (30 - x)P_2O_5$ system increased with increasing B_2O_3 content. Fig. 2 shows the composition dependence of d.c. conductivity in the glasses of $70V_2O_5 \cdot xB_2O_3 \cdot (30 - x)P_2O_5$. The conductivity of $70V_2O_5 \cdot 15B_2O_3 \cdot 15P_2O_5$ glass increased by a factor of about 10 in comparison with $70V_2O_5 \cdot 30P_2O_5$ glass. The activation energy for electric conduction (ΔH_{dc}) can be obtained from Equation 1. ΔH_{dc} of all the glasses was about 0.33 eV. This value corresponded to the hopping conduction of $V^{4+} \rightleftharpoons V^{5+}$. The pre-exponential factor (σ_0) in the conductivity shows the following Equation

$$\sigma_0 = \frac{\nu_{ph} e^2 \cdot c(1 - c)}{R_d kT} \exp(-2\alpha R_d) \quad (2)$$

where ν_{ph} is the phonon frequency, e the electric charge, c the valence ratio of vanadium ($V^{4+}/V^{4+} + V^{5+}$), and R_d the distance between vanadium ions. The factors, except for R_d and c, are almost constant in the range of whole composition. The change of V^{4+} (c) with the composition show inverse change on the conductivity and its change is very small. Therefore the distance of R_d have important effect on the conductivity. We reported that the phase separation of amorphous BVO_4 increased with increasing B_2O_3 content from observation of electron microscope [7, 8]. This indicates that the V_2O_5 concentration in a matrix and the conductivity increase with decreasing R_d.

3.2. Infrared absorption

Fig. 3 shows IR absorption spectra to confirm the

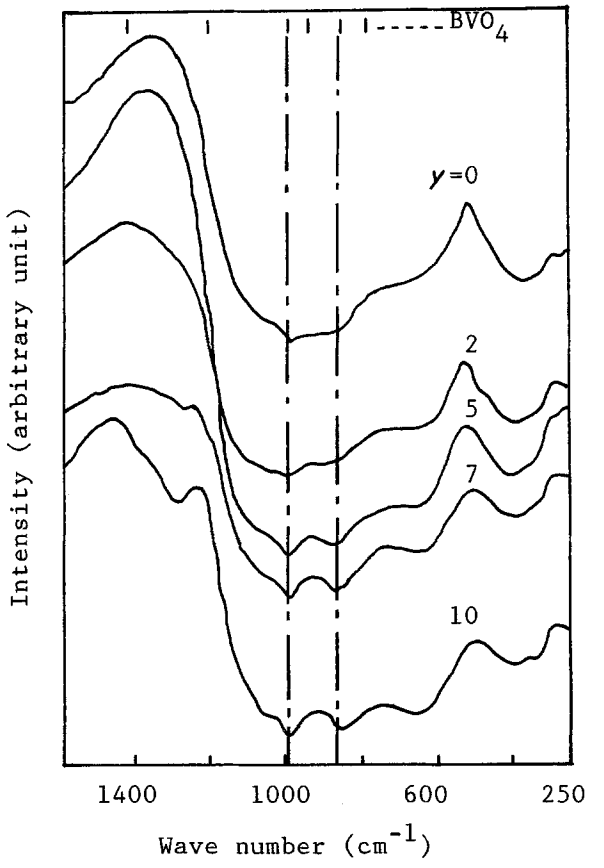

Figure 3 IR spectra in the glasses of $70V_2O_5 \cdot yB_2O_3 \cdot (30 - x)P_2O_5$.

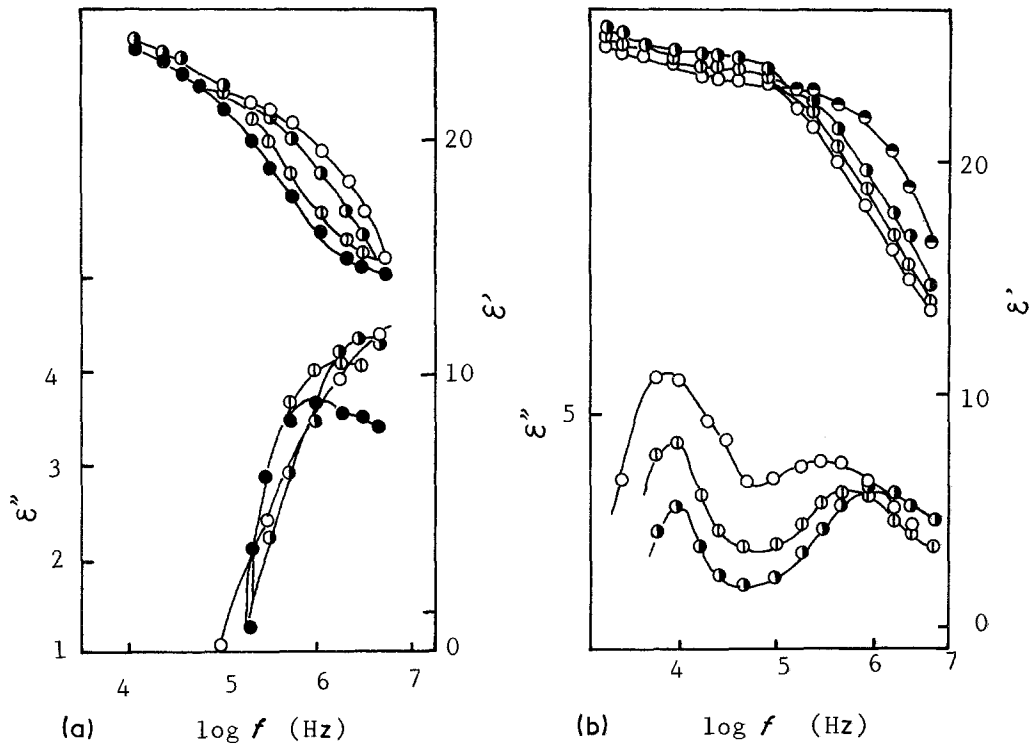

Figure 4 Frequency dependence of ε' and ε'' in the glasses of (a) $70V_2O_5 \cdot 30P_2O_5$ (● 35°C, ◐ 48°C, ◑ 76°C, ○ 94°C) and (b) $70V_2O_5 \cdot 2B_2O_3 \cdot 28P_2O_5$ (○ 31°C, ◐ 39°C, ◑ 53.2°C, ◓ 81°C).

phase separation of BVO_4. The absorption of BVO_4 appearing at 880 cm^{-1} increased with increasing B_2O_3 content. This result indicates that the phase separation of amorphous BVO_4 increases with increasing B_2O_3 content, similar to those observations of electron microscopy.

3.3. Dielectric properties

Figs 4a and b show the frequency dependence of both dielectric constant (ε') and dielectric loss (ε'') in the glasses of $70V_2O_5 \cdot 30P_2O_5$ and $70V_2O_5 \cdot 2B_2O_3 \cdot 28P_2O_5$. Dielectric loss ($\varepsilon''$) of left-hand figure showed a one peak and that of right-hand figure showed two peaks in the measurement range. The intensity of low frequency peak of left figure increased with increasing the phase separation. In both cases, the peak position moved toward higher frequency side with increasing temperature. Frequency (f_{max}) for the maximum dielectric loss (ε'') and inverse of the corresponding temperature ($1/T$) were found in parallel relation and are expressed as

$$f_{max} = f_{m_0} \exp\left(-\frac{\Delta H_{ac}}{RT}\right) \quad (3)$$

The activation energy for dielectric relaxation (ΔH_{ac}) was obtained from Equation 3. Table I shows ΔH_{ac} calculated from the equation. From these results, the peak of the left-hand figure corresponded to that of high frequency side of the left-hand figure. These peaks are assumed to result from hopping in relation to polaron and that of low frequency side is assumed to result from interface polarization between the phase separation and the matrix [7, 8].

3.4. V_2O_5 content dependence of internal friction

Fig. 5a shows the temperature dependence of internal friction in the glasses of $(50–80)V_2O_5 \cdot (50–20)P_2O_5$ system. Fig. 5a has been arranged to show each spectrum individually by shifting the appropriate spectra

TABLE I Glass composition, valence ratio, internal friction data and activation energy

Composition (mol %)	Ratio $V^{4+}/V^{4+} + V^{5+}$	Internal friction		ΔH_m (eV)	ΔH_{ac} (eV)	ΔH_{dc} (eV)
		Peak temperature (°C)	Peak area			
$50V_2O_5 \cdot 50P_2O_5$	0.530	203	1.00	0.39	0.41	0.40
$60V_2O_5 \cdot 40P_2O_5$	0.300	156	0.95	0.38	0.38	0.39
$70V_2O_5 \cdot 30P_2O_5$	0.056	118	0.80	0.32	0.33	0.35
$80V_2O_5 \cdot 20P_2O_5$	0.046	35	0.61	0.32	0.33	0.33
$70V_2O_5 \cdot 2B_2O_3 \cdot 28P_2O_5$	0.045	100	0.67	0.31	0.31	0.35
$70V_2O_5 \cdot 5B_2O_3 \cdot 25P_2O_5$	0.043	50	0.61	0.33	0.34	0.35
$70V_2O_5 \cdot 7B_2O_3 \cdot 23P_2O_5$	0.038	35	0.44	0.33	0.32	0.35
$70V_2O_5 \cdot 10B_2O_3 \cdot 20P_2O_5$	0.034	0	0.38	0.32	0.31	0.35
$70V_2O_5 \cdot 15B_2O_3 \cdot 15P_2O_5$	0.027	−20	0.13	0.32	0.32	0.34

ΔH_m is the activation energy of internal friction (eV).
ΔH_{ac} is the activation energy of dielectric relaxation in high frequency peak (eV).
ΔH_{dc} is the activation energy of d.c. conductivity (eV).

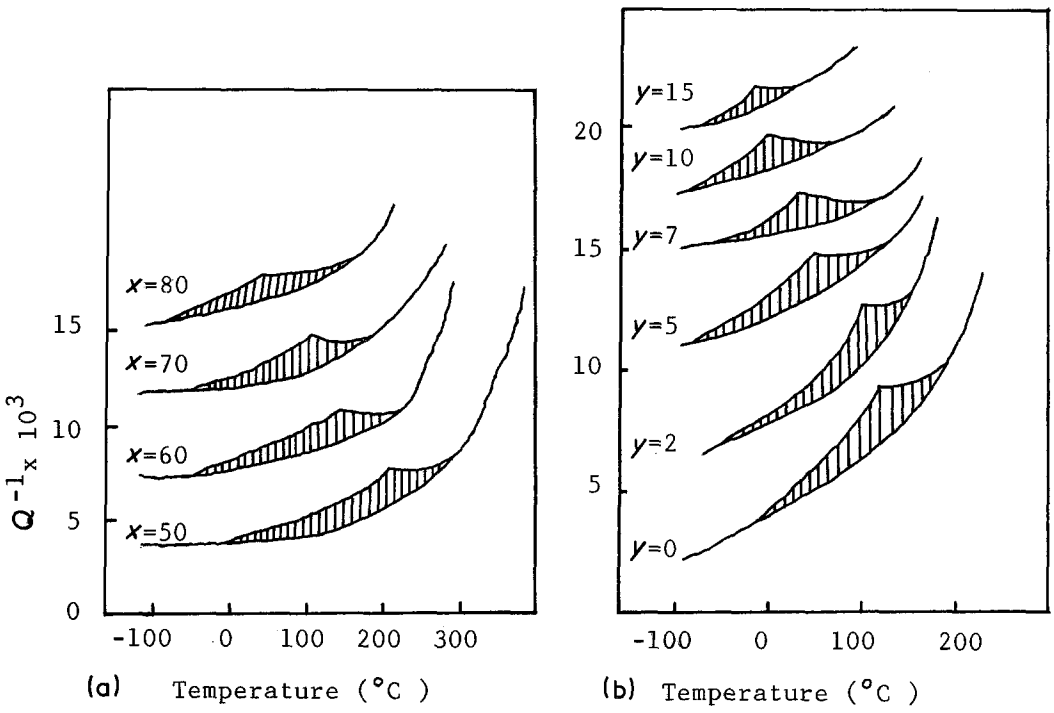

Figure 5 Temperature dependence of internal friction in the glasses of (a) $xV_2O_5 \cdot (100 - x)P_2O_5$ and (b) $70V_2O_5 \cdot yB_2O_3 \cdot (30 - x)P_2O_5$.

upward. One peak was observed in the measurement range for all glasses. The peak area decreased with increasing V_2O_5 content. This result is due to the contribution of decreasing R ratio than increasing V_2O_5 content. The peak temperature shifted toward the low temperature side with increasing V_2O_5 content. This is consistent with the tendency that the glasses of high V_2O_5 content have high conductivity.

3.5. B_2O_3 content dependence of internal friction

Fig. 5b shows the temperature dependence of internal friction in the glasses of $70V_2O_5 \cdot xB_2O_3 \cdot (30 - x)$-$P_2O_5$. Fig. 5b has been arranged to show each spectrum individually by shifting the appropriate spectra upward. One peak was observed in the measurement range for all glasses. The peak shifted toward the low temperature side with increasing B_2O_3 content and the peak area decreased. Fig. 6 shows the dependence of B_2O_3 content on peak temperature and ratio of peak area. The ratio of peak area showed a relative ratio when the peak area of internal friction in the glass of $70V_2O_5 \cdot 30P_2O_5$ was normalized as unity. The peak temperature of the internal friction and peak area decreased with increasing B_2O_3 content. The decrease of peak area can be seen in other words as the decrease of energy loss. That is, amorphous BVO_4 increased with increasing B_2O_3 content and the distance between the vanadium ions in the matrix decreased inversely. Therefore the hopping conduction energy of glasses containing B_2O_3 are less than glasses not containing B_2O_3. For the general evaluation of the peak area for various glasses with different R ratio, indexing is effective. In this report, we applied the method, as shown in Fig. 7, a closed circle indicates the measured value of internal friction ($Q^{-1} \times 10^3$), and an open circle indicates the base line calculated by Lagrange's interpolation method [19]. By reduction of the calculated value from the measured value, a spectrum is obtained as shown in the lower curve in Fig. 7. This spectrum indicates the simple temperature dependence of the relaxation phenomenon, which was excluded with the rise of the glass network. The peak area was calculated by Simpson's rule using trapezoids.

3.6. Peak area of internal friction and R ratio

R ratio-dependent peaks were observed not only in iron phosphate glass, but also in vanadium phosphate glasses and phase-separating vanadium borophosphate glasses. With regard to these three sorts of glasses, the peak area of internal friction was indexed as the division of peak area by mole number, and such indices were further changed to relative values, which were

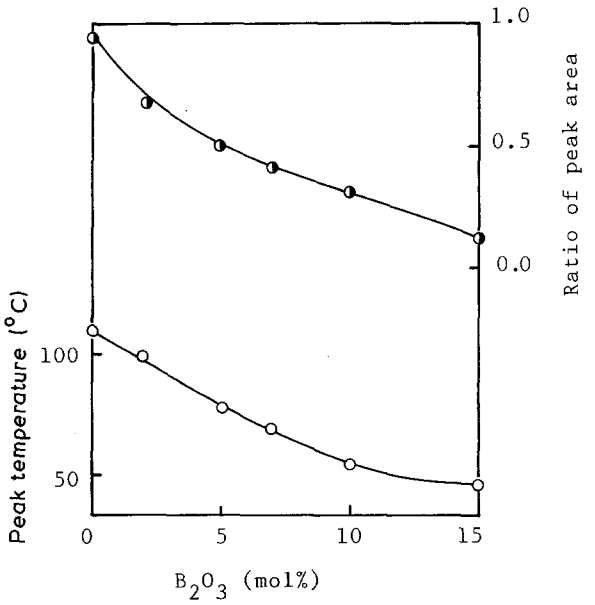

Figure 6 Compositional dependence of peak temperature (○) and peak area (◑) on internal friction with B_2O_3 content.

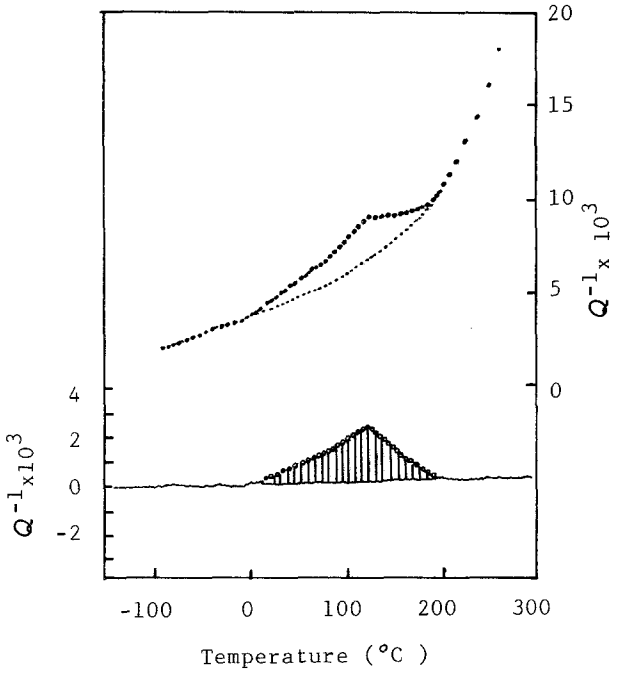

Figure 7 Base line by Lagrange's interpolation method for peak area of internal friction in the glass of $70V_2O_5 \cdot 30P_2O_5$ (● measured value, ○ calculated value).

plotted in Fig. 8, showing their R ratio dependence. All the points coincided with the normalized curve with a maximum at $R = 0.5$. It has been proved that the peak area of internal friction is dependent on the carrier concentration, as shown in Fig. 8, and is independent of the sort of transition metal.

3.7. Frequency dependence of internal friction

Fig. 9 shows the measured results of internal friction at different frequencies in the $70V_2O_5 \cdot 30P_2O_5$ and $70V_2O_5 \cdot 10B_2O_3 \cdot 20P_2O_5$ glass. Along with the increase

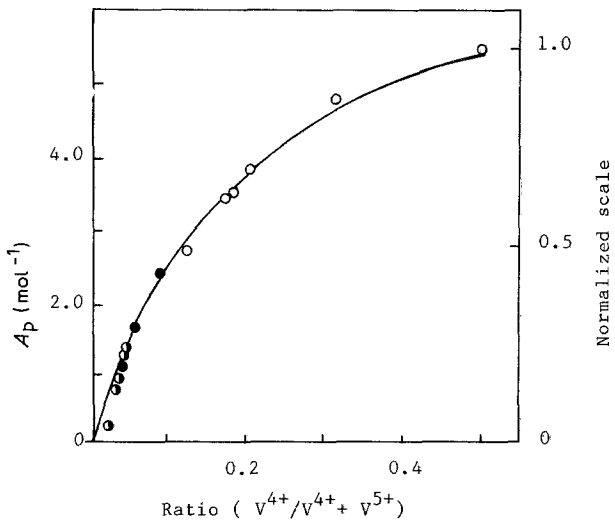

Figure 8 Valence ratio (R) dependence of peak area (A_p)/mol of internal friction. (○ $Fe_2O_3 \cdot P_2O_5$ series, ● $V_2O_5 \cdot P_2O_5$ series, ◑ $V_2O_5 \cdot B_2O_3 \cdot P_2O_5$ series).

in frequency, the temperature showing the peak shifted toward the higher temperature side. The maximum peak temperature and frequency were linearly related. The activation energy was calculated for both dielectric loss and internal friction by Equation 2. The activation energy for both had the same value of about 0.33 eV. This indicates that observed peak on internal friction is due to the electronic hopping between $V^{4+} \rightleftarrows V^{5+}$, corresponding to the observed peak for the dielectric relaxation phenomenon.

3.8. Generation mechanism of internal friction peak

For the glasses containing transition metal oxide, an electron is trapped in the polarization field and is restricted from free movement, thus forming a polaron. In order to mobilize the localized electrons on V^{4+},

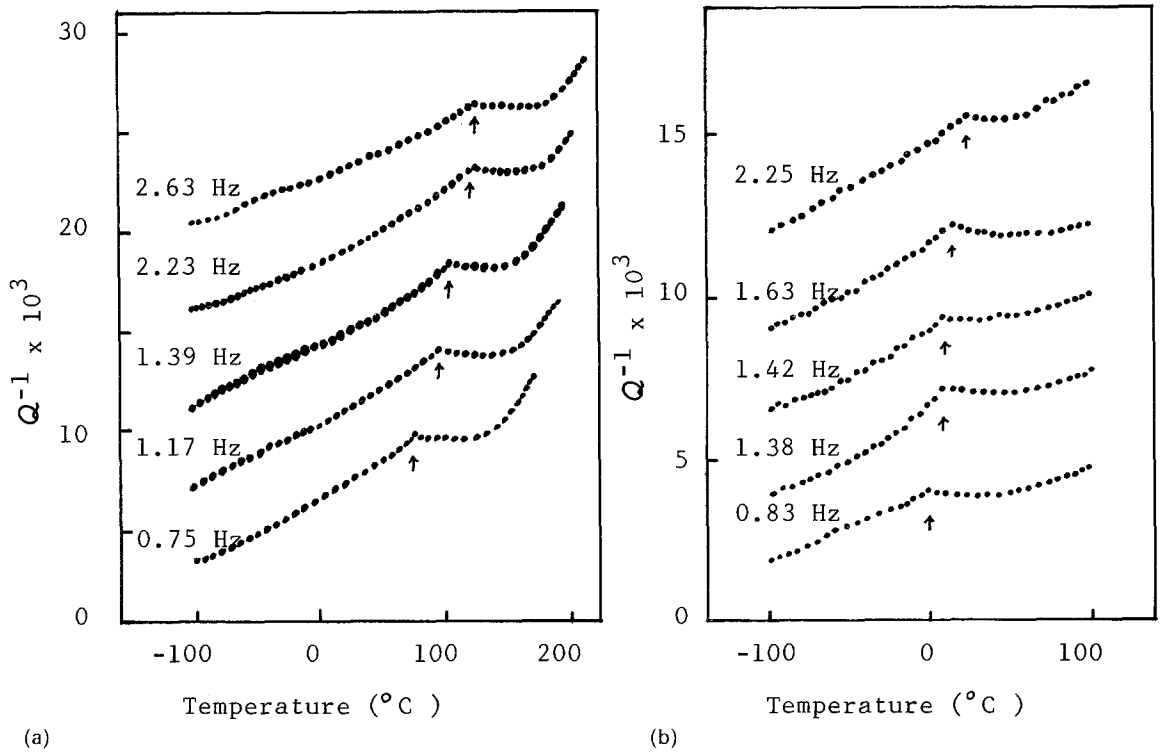

Figure 9 Peak shift of internal friction by various frequencies in the glasses of (a) $70V_2O_5 \cdot 30P_2O_5$ and (b) $70V_2O_5 \cdot 10B_2O_3 \cdot 20P_2O_5$.

the aid of lattice oscillation is required. In this circumstance, electrons are not considered to move by themselves, but by the hopping motion activated by lattice oscillation. In the case of electron-conductive glass, it is assumed that the specimen is given a dynamic strain by torsion elastic energy, which is caused by the oscillation of the pendulum, and the energy levels change. This change of energy level and thermal activation process together induce the hopping in relation to the polaron and cause the internal friction, which in turn results in more violent lattice oscillation.

4. Conclusion

In the experiments in the glasses of $(50–80)V_2O_5 \cdot (50–30)P_2O_5$ and $70V_2O_5 \cdot xB_2O_3 \cdot (30 - x)P_2O_5$ system, electrical properties (d.c. conductivity, dielectric relaxation) and internal friction were measured, and the following results were obtained.

(1) The activation energy calculated from internal friction peak and dielectric loss peak has the same value of about 0.33 eV. This indicates that the observed peak on internal friction is due to the electronic hopping between $V^{4+} \rightleftharpoons V^{5+}$, corresponding to the observed peak for the dielectric relaxation phenomenon.

(2) In defining f_{max} as the frequency to show maximum peaks of both dielectric relaxation and internal friction, the figures of f_{max} plotted against $1/T$ were found to lie on a parallel line. This indicated that the frequencies f_{max} corresponded to dielectric relaxation and to internal friction which had the same activation energy (0.33 eV) as that of d.c. conductivity.

(3) For three sorts in the glasses of $40Fe_2O_3 \cdot 60P_2O_5$, $(50–80)V_2O_5 \cdot (50–30)P_2O_5$ and $70V_2O_5 \cdot xB_2O_3 \cdot (30 - x)P_2O_5$ system, indices of peak area divided by mole number of transition metal ion which were plotted against R ratio were found to lie on a certain normalized curve, which implied that the peak area was dependent on the R ratio in a certain rate, independently of the sort of transition metal. The reason of internal friction was considered to be as follows. Firstly, dynamic strain is applied to the specimen; secondly, the energy level between the localized levels changes; thirdly, this change and thermal activation process jointly induce the hopping in relation to polaron; and finally, the internal friction results.

References

1. M. MUNAKATA, *Solid State Electron* **1** (1960) 159.
2. N. F. MOTT, *J. Non-Cryst. Solids* **1** (1968) 1.
3. M. SAYER, A. MANSINGH, J. M. REYES and G. ROSENBLATT, *J. Appl. Phys.* **42** (1971) 2857.
4. A. FELTZ, *J. Non-Cryst. Solids* **72** (1985) 335.
5. M. SAYER, *ibid.* **58** (1983) 91.
6. V. J. WASYLAK, J. KOPROWSKI, E. CZERWOSZ, W. WARSCHAV, E. S. KRAKAU, *Glass Technische Berichte* **57** (1984) 12.
7. Y. HAKAMATSUKA, N. YONEDA and T. TSUCHIYA, *J. Ceram. Soc. Jpn* **89** (1981) 461.
8. *Idem, ibid.* **90** (1982) 56.
9. E. H. VERSTEGEN and DELBERT E. DAY, *J. Non-Cryst. Solids* **14** (1974) 142.
10. M. IMAOKA and H. SAKAMURA, *J. Ceram. Soc. Jpn* **87** (1979) 387.
11. H. SAKAMURA, M. TOTSUKA, I. YASUI and M. IMAOKA, *ibid.* **89** (1981) 603.
12. W. CHOMKA, O. GZOWSKI, L. MURAWSKI and D. SAMATOWICTZ, *J. Phys. C* **11** (1978) 3081.
13. A. K. BANDYOPADHYAY, J. PHALIPPOU and J. ZARZYCKI, *J. Non-Cryst. Solids* **57** (1983) 41.
14. W. CHOMKA, D. SAMATOWICZ, O. GZOWSKI and L. MURAWSKI, *J. Mater. Sci. Lett.* **1** (1982) 264.
15. W. CHOMKA and D. SAMATOWICZ, *J. Non-Cryst. Solids* **57** (1983) 327.
16. W. CHOMKA, O. GZOWSKI, L. MURAWSKI and D. SAMATOWICZ, *J. Mater. Sci. Lett.* **1** (1982) 264.
17. T. TSUCHIYA, M. OTONARI and T. ARIYAMA, *J. Ceram. Soc. Jpn Int. Edn* **95** (1987) 267.
18. *Idem, J. Ceram. Soc. Jpn* **95** (1987) 295.
19. M. HIRATA and S. SERIZAWA, "Application Mathematics for Chemical Technologist" (Maruzen, Japan, 1976) pp. 19–45.

Received 21 December 1987
and accepted 6 May 1988